Technical Notes

TECHNICAL NOTES are short manuscripts describing new developments or important results of a preliminary nature. These Notes cannot exceed 6 manuscript pages and 3 figures; a page of text may be substituted for a figure and vice versa. After informal review by the editors, they may be published within a few months of the date of receipt. Style requirements are the same as for regular contributions (see inside back cover).

Porous Airfoils in Transonic Flow

G. Savu* and O. Trifu*
National Institute for Scientific and Technical Creation INCREST, Bucharest, Romania

Nomenclature

C_D = drag coefficient
C_F = friction drag coefficient
C_p = pressure coefficient
M_∞ = freestream Mach number
p = pressure
p_p = plenum chamber pressure
Q = mass rate through porous surface
s = length of the porous zone
U_∞ = freestream velocity
u,v = perturbation velocity components
u_p = perturbation velocity in the plenum chamber
v_n = normal filtration velocity
x,z = Cartesian coordinates
$x_{1,2}$ = limits of the porous region
Z = airfoil ordinate
Z' = airfoil contour's slope
Δp = pressure gradient through porous surface
γ = ratio of the specific heats
φ = perturbation potential
ρ_∞ = freestream density
σ = porosity
$\bar{\sigma}$ = nondimensional porosity factor

Introduction

THE most serious inconvenience of supercritical airfoils is the narrowness of the optimum Mach number and incidence range.[1]

In this Note, a method leading to shockless supercritical flow around the airfoil in a broader transonic Mach number range is proposed. As is well known, in order to reduce blockage (see Ref. 2), the walls of the test section of a transonic wind tunnel are perforated. If the region of the airfoil surface where the shock waves occur is perforated (see Fig. 1), the internal cavity of the airfoil is similar to the plenum chamber of a transonic wind-tunnel test section.

The use of porous surface airfoils has been proposed by Carafoli,[3] Rahmatulin,[4] Patraulea,[5] and Ventres and Barakat,[6] but all of these authors assumed that the airfoil was thin (represented by its meanline) and calculated only the pure subsonic or pure supersonic regimes.

The analysis undertaken in the present Note demonstrates that the pressure jump (shock wave) intensity on thick airfoils in the transonic regime is considerably reduced by setting up a secondary flow through the porous surface (between the external region and the internal cavity of the airfoil) in both directions. Such a secondary flow is subjected to the Darcy law, which states that the normal velocity on a porous surface is proportional to the pressure gradient between its two sides.

Received July 28, 1982; revision received Jan. 14, 1983.

*Research Scientist, Aerodynamics Department.

Analysis

The governing equation, which describes the flow around the airfoil, is the well-known von Kármán inviscid, small-disturbance partial differential equation for the perturbation potential φ,

$$(1-M_\infty^2)\varphi_{xx} - (\gamma+1)\cdot M_\infty^2 \varphi_x \varphi_{xx} + \varphi_{zz} = 0 \tag{1}$$

The boundary conditions on the airfoil surface are:
1) Zero normal velocity on the solid regions

$$v_n = 0 \tag{2}$$

2) Normal velocity value deduced from Darcy's law on the porous regions

$$v_n = \sigma \Delta p \tag{3}$$

$$\sigma = \bar{\sigma}/\rho_\infty U_\infty \tag{4}$$

The porosity factor $\bar{\sigma}$ is a function of the hole size and distribution on the surface. Wire sieves or perforated plates (see Fig. 1) may be used to insure the desired porosity. Experimental and theoretical results concerning the porosity factor of such systems are given in the literature.[5,7]

Two different situations may be considered for the secondary flow through the porous wall of the airfoil:

1) It is assumed that inside the airfoil the pressure is equal to the static pressure of the freestream p_∞-ventilated cavity. This is made possible by connecting the cavity inside the airfoil to p_∞ through a separate pipe. Because the airfoil's internal cavity has an external (p_∞) air supply for the correct fulfillment of the infinity flow conditions, the continuity condition on a control surface around the airfoil requires the existence of positive or negative source-type singularities placed on the airfoil's meanline along its porous region.

2) If no special connection is established between the internal airfoil cavity and the freestream-unventilated cavity, the pressure inside the cavity differs from p_∞ and its value p_p is calculated as shown below. This cavity pressure is a result of the mutual interaction between the external flow and the flow inside the cavity: the fluid (air) flows in through some of the orifices and flows out from the cavity through others in

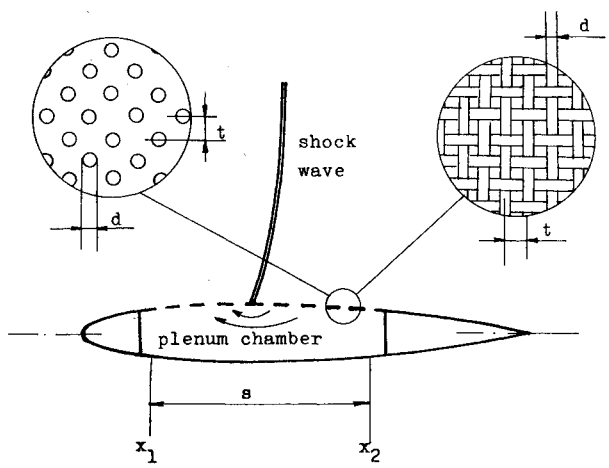

Fig. 1 Porous airfoil: a) with perforated plate, b) with wire sieve.

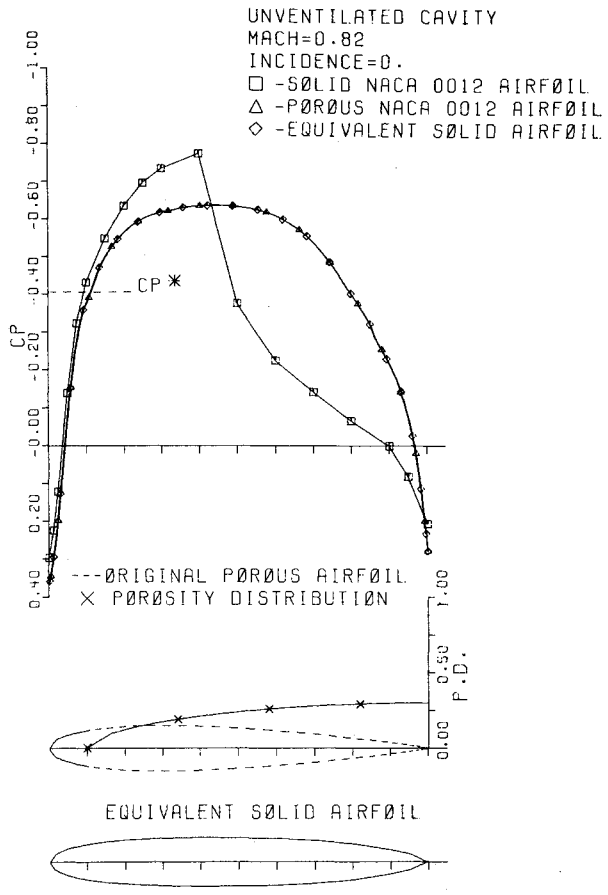

Fig. 2 Pressure distributions for $M_\infty = 0.82$ on the original solid, porous, and equivalent solid airfoils; 0.3 maximum porosity factor located at the trailing edge, $p_p \neq p_\infty$.

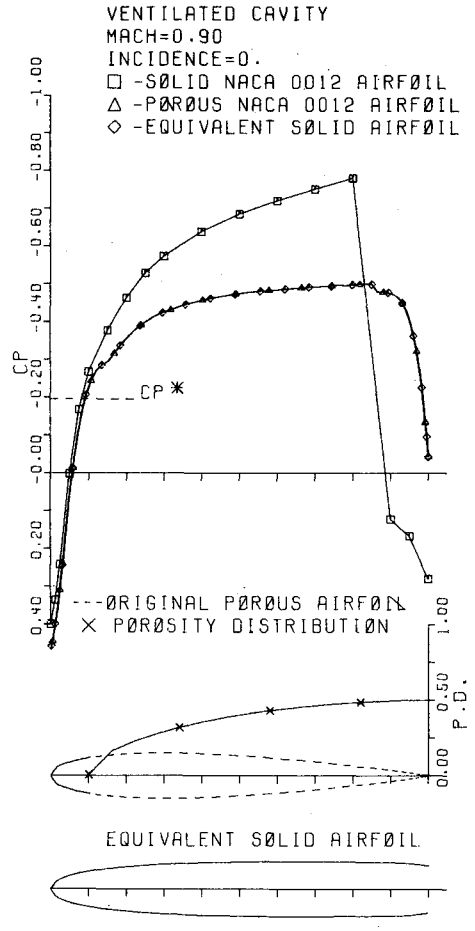

Fig. 3 Pressure distributions for $M = 0.90$ on the original solid, porous, and equivalent solid airfoils; 0.5 maximum porosity factor located at the trailing edge, $p_p = p_\infty$.

such a way that the global mass rate over the entire porous region is zero, as

$$Q = \int_s \rho v_n \mathrm{d}s = 0 \tag{5}$$

For both situations, in the small-disturbances theory the boundary condition on the airfoil is written in the form,

$$v_{Z=0} = (U+u)Z' + \tilde{\sigma}(u-u_p) \tag{6}$$

where

$$u_p = 0 \tag{7}$$

for situation 1, and

$$u_p = \int_s \rho u \tilde{\sigma} \mathrm{d}s \Big/ \int_s \rho \tilde{\sigma} \mathrm{d}s \tag{8}$$

deduced from Eq. (5), for situation 2.

Equation (1), associated with the boundary conditions [Eq. (6)], was numerically solved with the aid of a FORTRAN computer code SG58A, described in Ref. 8. Using an expanded mesh with unequal steps, the differential operator [Eq. (1)] was written in finite differences, and a system of nonlinear algebraic equations in the $\varphi_{i,j}$ unknowns was obtained. For the elliptic case ($M<1$) centered differences were employed and for the hyperbolic case ($M>1$) upwind differences.[9] In order to solve the equation system with the boundary conditions of Eq. (6), an iterative Newton-Raphson procedure was applied.

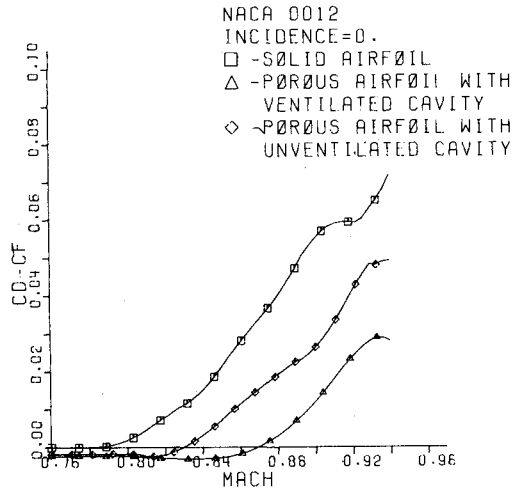

Fig. 4 Drag coefficient (without friction) variation vs M_∞.

With the aid of a second-order integration formula, the pressure distribution resulting from the analysis procedure applied to the porous airfoil was used to obtain an equivalent solid airfoil. This new solid equivalent airfoil (see Figs. 2 and 3) was subjected to the analysis procedure. The resultant pressure distribution was practically the same as on the original airfoil (i.e., shockless).

Results and Conclusions

The flow over a NACA 0012 airfoil at zero incidence and various transonic Mach numbers was numerically studied.

Numerical experiments did show that it is better to use a gradual variation of the porosity factor going from $\bar{\sigma}=0$ on the solid region to $\bar{\sigma}=\bar{\sigma}_{max}$ on the maximum porosity region of the airfoil. Thus, the following porosity distribution function was adopted:

$$\bar{\sigma}=\bar{\sigma}_{max}\sqrt{\sin\left(\pi\frac{x-x_1}{x_2-x_1}\right)} \tag{9}$$

In order to obtain the desired pressure distribution on the airfoil, any porosity distribution function may, in principle, be used. This also makes the method appropriate as a design procedure.

The graphically represented pressure distributions show that on the porous airfoil the flow is shockless. This important feature is maintained over a quite large Mach number domain as can be seen from the C_D-C_F curves plotted against Mach number in Fig. 4 for the same porosity distribution. A sensible increase in the Mach drag rise number is visible for the porous airfoil, especially in the case of a ventilated cavity. In the numerical experiments, an important fact was observed: for the subcritical Mach numbers the influence of the porosity on the pressure distribution is negligible.

These theoretical results, obtained in the small-disturbance, steady, inviscid flow theory are promising. They must be verified with a more complete flow model (including viscosity effects) and especially by comparison with experimental data.

References

[1]Bauer, F., Garabedian, F., and Korn, D., "Supercritical Wing Sections, III," *Lecture Notes in Economics and Mathematical Systems*, No. 150, Springer-Verlag, Berlin, Heidelberg, New York, 1977, pp. 82-83.

[2]Dumitrescu, L. Z. and Savu, G., "Influence de l'écoulement dans les chambres plénum sur les corrections d'essais en souffleries transsoniques," IMFCA Report, 1977.

[3]Carafoli, E., "On a Permeable Lifting Surfaces Theory," *Lucrarile Sesiunii Generale Stiintifice din 2-12 iunie 1950*, Editura Academiei, Romanian Peoples Republic, 1951.

[4]Rahmatulin, H. A., "Perforated Aerodynamic Shapes," *Vestnik Moskovskovo Universiteta*, No. 3, 1950, p. 41.

[5]Patraulea, N. N., "Aerodynamics of the Porous Surfaces," Editura Academiei, Romanian Peoples Republic, 1956, pp. 26-32.

[6]Ventres, C. S. and Barakat, R., "Aerodynamics of Airfoils With Porous Trailing Edges," *The Aeronautical Quarterly*, Vol. XXX, Pt. 2, May 1979, pp. 387-399.

[7]Ovchinnikov, O. N., "The Perforated Flat Plate in Stabilized Viscous Flow," *Mechanika Zhidkosti i Gaza*, Nov.-Dec. 1966, pp. 65-73.

[8]Savu, G., "A Computer Program for 2D Transonic Flow in Small Disturbances Theory Calculation 222SG58A," INCREST, 1981.

[9]Murman, E. M. and Cole, J. D., "Calculation of Plane Steady Transonic Flow," *AIAA Journal*, Vol. 9, Jan. 1971, pp. 114-121.

Higher Order Strip Integral Method for Three-Dimensional Boundary Layers

K. Kurian Mani*
Lockheed California Company, Burbank, California

Nomenclature

I_j = influence coefficients
N = number of strips
R_e = Reynolds number based on velocity outside the boundary layer
U,V = X and Y components of velocity outside the boundary layer
u,v = X and Y components of velocity inside the boundary layer
X,Y,Z = coordinate directions
η = Z/δ_{11} *or* Z/δ_{22}; nondimensional coordinate in Z direction
δ_{11},δ_{22} = boundary-layer thicknesses in the X and Y directions, respectively
δ_1,δ_2 = displacement thicknesses along and normal to external streamline direction
θ_1,θ_2 = momentum thicknesses along and normal to external streamline direction

Superscript

$( )'$ = differentiation with respect to η

Subscripts

$,( )$ = derivative with respect to the accompanying quantity
e = reference quantity at edge of boundary layer
n = component perpendicular to external flow
t = component parallel to external flow
L = upper bound of integration
∞ = reference quantity at freestream

Submitted Oct. 18, 1982; revision received Oct. 21, 1983.

*Research Specialist. Member AIAA.

Introduction

THE design of aircraft wings and other similar lifting surfaces is highly influenced by the boundary layer over the surface. Two-dimensional boundary layers can be calculated relatively easily. Computation of three-dimensional boundary layers is difficult and time consuming. A recent study by Humphreys[1] showed that the current methods for the computation of three-dimensional boundary layers lack accuracy, even when the cross flow is small. Yet another study by Lemmerman[2] showed that there exists a considerable degree of scatter in the results by finite difference methods. Three-dimensional computations usually take large computational time, especially if finite difference methods are used. In practical applications the boundary-layer codes form an intermediate part of a much larger program along with a potential flow code. An iterative solution between these two analyses utilizes a large amount of computing resources before convergence. The integral methods similar to that by Stock[3] are more attractive than finite difference methods in this respect. These methods are based on parametric representation of velocity profiles and are expected to give good results when the real flowfield is a subset of the chosen class of assumed profiles. Three-dimensional boundary layers consist of a wide variety of profiles, and parametric representation may not always be possible. Strip integral methods offer an alternative to solve this problem. The boundary layer can be assumed to be divided into a few strips with the velocity profiles varying according to a simple power law between the strips. This approach provides a large degree of flexibility by eliminating the need for assumed profiles. Moreover, the velocity profiles can be predicted, if needed, by choosing a large number of strips. A variety of boundary layers can be studied with a wide spectrum of differing velocity profiles. The more complex the flow, the greater the number of strips required for computation.

In order to study the feasibility of such an approach, a laminar flow problem with large cross flows was chosen. Loos[4] has solved the three-dimensional laminar boundary layer formed due to parabolic streams over a flat plate. The results obtained by the application of strip integral method to the above problems is found to be very encouraging. The details of the method are briefly described below.